

pubs.acs.org/cm Methods/Protocols

# Determining the Absolute Anodic Stability Threshold of Polymer Electrolytes: A Capacity-Based Electrochemical Method

Zhuo Li, Yineng Zhao, and Wyatt E. Tenhaeff\*



Cite This: Chem. Mater. 2021, 33, 1927-1934



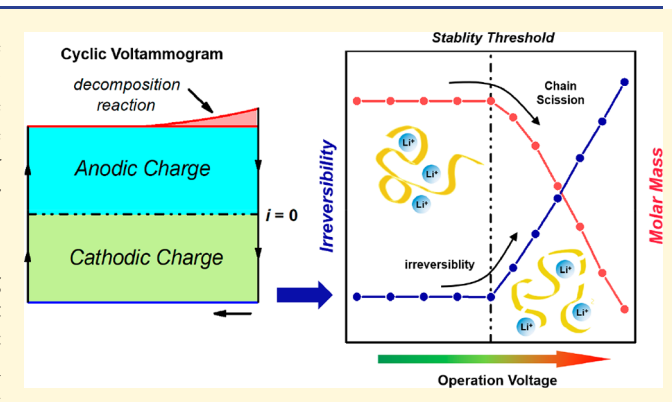
**ACCESS** 

III Metrics & More

Article Recommendations

Supporting Information

ABSTRACT: Inherently safe, reversible, energy-dense solid-state lithium metal batteries require solid electrolytes that are electrochemically compatible at the high potentials of the cathode. In the scientific literature, there are significant discrepancies in the reported anodic stabilities of solid-state electrolytes, especially polymeric materials. Addressing the limitations of popular characterization approaches, such as linear sweep voltammetry, this study introduces a capacity-based electrochemical method, termed the reversibility test, as a reliable alternative in determining the anodic stability of polymer electrolytes. The reversibility test integrates the anodic and cathodic currents during a cyclic voltammetry measurement to identify irreversibility ( $\rho$ ) through the capacity ratios. The capacity ratio is unchanged when the



electrolyte is electrochemically stable but deviates at potentials exceeding the electrolyte's stability threshold. Using this reversibility test, the anodic stabilities of poly(ethylene oxide) (PEO) and hydrogenated nitrile butadiene rubber (HNBR), both blended with lithium bis(trifluoromethanesulfonyl) imide (LiTFSI), were determined to be 3.6 and 3.7 V vs Li/Li<sup>+</sup>, respectively. The stability threshold of PEO is validated by size exclusion chromatography. At charge potentials exceeding 3.6 V, the  $\bar{M}_{\rm W}$  of PEO monotonically decreases, indicating further oxidation. Thus, the reversibility test is established as a sensitive and versatile characterization method for determining the oxidative stability of polymer electrolytes.

#### 1. INTRODUCTION

Successful deployment of practical dense electrochemical energy storage requires inherently safe cell designs, motivating intense interest in solid-state lithium batteries. The simultaneous push toward higher cell potentials to maximize energy densities has revealed critical challenges associated with cathode/electrolyte interfacial stability. 1,2 Long-term, reversible cycling of an electrochemical cell requires that the electrolyte be electrochemically stable, making determination of the potential stability window of solid electrolytes a critical task in solid-state battery development.3-6 The practical stability window of solid electrolytes is often described by a single voltage threshold referenced relative to Li/Li<sup>+</sup>, which is measured by the linear sweep voltammetry of a cell with an inert working electrode and Li counter/reference electrode. Common choices for the working electrode include noble metals (e.g., Au and Pt), various forms of carbon (vitreous carbon, highly oriented pyrolytic graphite, etc.), and stainless steel (SS). The threshold potential is determined at an arbitrary current density or at the intersection of two extrapolated trend lines for the stable low voltage regions and oxidatively unstable higher voltages.

However, these approaches are often applied inconsistently, resulting in significant discrepancies in the literature. For example, the oxidative stability for polymer electrolytes based

on poly(ethylene oxide) (PEO) has been reported as low as 3.8 V and up to 5.7 V vs Li/Li<sup>+,9-16</sup> For other solid-state electrolytes such as Li<sub>7</sub>La<sub>3</sub>Zr<sub>2</sub>O<sub>12</sub>(LLZO) and Li<sub>10</sub>GeP<sub>2</sub>S<sub>12</sub>(LGPS), the reported voltage stabilities range from 4.0 to 9.0 V and 2.1 to 4.0 V vs Li/Li<sup>+</sup>, respectively. 17-22 The accuracy of the LSV method is particularly unsatisfactory in determining the stability threshold of polymeric electrolytes. This is demonstrated with poly(ethylene oxide)/lithium bis(trifluoromethanesulfonyl) imide (PEO:LiTFSI), a polymer electrolyte archetype, in Figure 1a,b. Vitreous carbonl PEO:LiTFSIlLi cells were prepared in parallel and scanned at different rates. Interpretation of the voltammogram suggests that neither using a preset current density (in this case, 10  $\mu$ A/ cm<sup>2</sup>) nor extrapolating the "rapid increasing region" of the i-Ecurve provides theoretically meaningful or consistent stability thresholds.

Received: November 2, 2020 Revised: February 22, 2021 Published: March 3, 2021





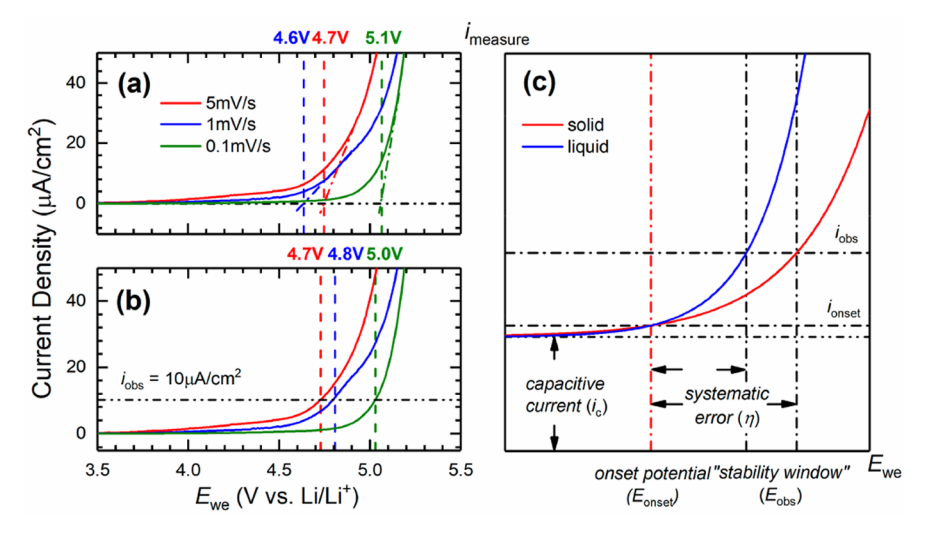


Figure 1. Linear sweep voltammogram of PEO:LiTFSI (O/Li = 10) from 3.5 to 5.5 V vs Li/Li $^+$  at room temperature. Examples of "stability thresholds" determined by (a) extrapolating the voltammogram and (b) using an arbitrary onset current density. (c) Description of the systematic error in estimaing the oxidative stability from current-based methods.

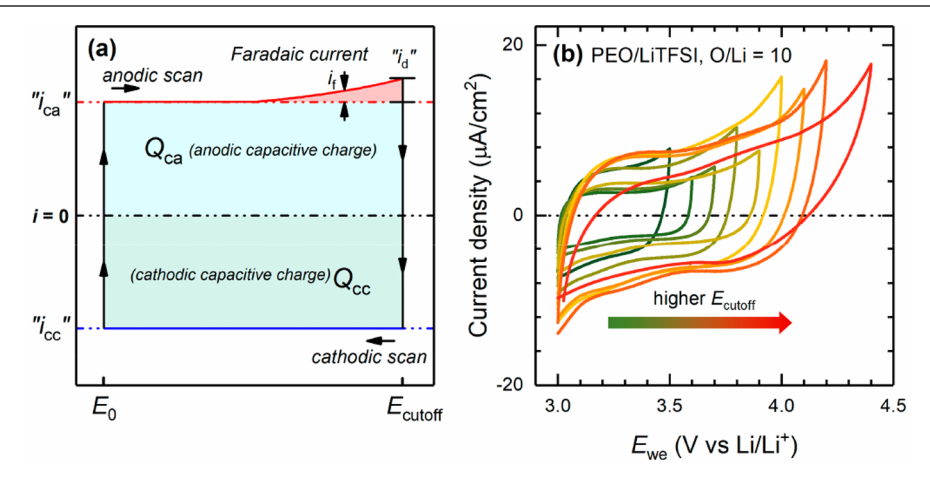


Figure 2. (a) Conceptual illustration of the various contributions to anodic and cathodic charge capacities in the reversibility test. The electrolyte is cycled between  $E_0$  and  $E_{\text{cutoff}}$  to form a closed envelop. (b) Cyclic voltammograms of PEO:LiTFSI:graphite = 21.5:14.0:64.5 (by mass) sample scanned from 3.0 V vs Li/Li<sup>+</sup> to various  $E_{\text{cutoff}}$  values at 60 °C and 0.1 mV/s rate.

The inconsistency of LSV is intrinsic to the method. Researchers have investigated this limitation of LSV in liquid-state systems; its arbitrariness has been criticized when an "onset" current density is chosen as a "practical standard". <sup>23,24</sup> For example, the current density is proportional to the electrolyte conductivity, making the comparison of electrolytes with differing conductivities problematic. Methods have been developed to improve the reliability of LSV for determining the anodic stability, such as linear fitting of the current—potential curve. <sup>8,25</sup> In undisturbed liquid systems with relatively fast diffusion, the voltammogram of a completely irreversible system is linear before and after the threshold potential. <sup>26</sup> Thus, an oxidation/reduction limit can be found by extrapolating the two linear regions.

This method of extrapolating the voltammogram to determine the stability thresholds requires that the oxidation reaction is not diffusion controlled, which is often violated in polymer electrolyte systems with diffusion coefficients characteristically lower than those in liquid electrolytes (e.g., in liquid alkyl carbonate electrolyte,  $D_{\rm Li}^+=2-4\times10^{-6}~{\rm cm}^2/{\rm s}$  and  $D_{\rm carbonate}=3-5\times10^{-6}~{\rm cm}^2/{\rm s}$ , and in PEO:LiTFSI  $D_{\rm Li}^+=1\times10^{-7-8}~{\rm cm}^2/{\rm s}$  and  $D_{\rm [EO]}=1\times10^{-10}~{\rm cm}^2/{\rm s}$ ). As a

result, the current density at comparable overpotential is several orders of magnitude smaller than that at liquid-state experiments. The limitation of mass transport not only causes difficulty in theoretical analysis but also results in a larger error for any current density-based method, illustrated in Figure 1c. Around the true stability threshold potential of the electrolyte  $(E_{\text{onset}})$ , the Faradaic current  $(i_{\text{onset}})$  may be indistinguishable from the capacitive current ( $i_{\rm C}$ ). A significant increase of the observed current density  $(i_{obs})$  is then required to make the assignment to a Faradaic reaction. The difference between  $i_{
m onset}$ and  $i_{\rm obs}$  is the systematic error  $\eta$ . In solid state systems, the slow kinetics and low diffusion coefficient will flatten the i-E curve; thus, a larger  $\eta$  is expected compared to those of liquid electrolytes.<sup>26</sup> Furthermore, the value of the systematic error depends on the shape of the voltammogram, making the error unique to each case and practically impossible to correct in repeated measurements and between samples. Thus, considerable inconsistency is expected to be inherent to the LSV of polymer electrolytes.

**Chemistry of Materials** Methods/Protocols pubs.acs.org/cm

# 2. THEORY OF THE ELECTROCHEMICAL REVERSIBILITY TEST

Given these limitations of current density-based techniques, an alternative method based on capacity measurements was developed. A capacity-based electrochemical method for determining the electrolyte stability window was first suggested by Xu et al., where the cell potential is repeatedly scanned from open circuit to a progressively higher upper potential limit (essentially cyclic voltammetry). <sup>23,24,31</sup> The charge capacities of the anodic and cathodic scans are compared. As the cell potential increases, the Faradaic current associated with the oxidation of the electrolyte contributes to anodic capacity. The ratio of anodic to cathodic capacity is a measure of the irreversibility of the process; this ratio was used to define the stability window of the electrolyte. This method was demonstrated with conventional aprotic liquid electrolytes.

A theoretical voltammogram of a sample scanned between  $E_0$  and  $E_{\text{cutoff}}$  is provided in Figure 2a. Theoretically, if no Faradaic reactions are contributing to the current and the capacitive, non-Faradaic current is fully reversible, the charge capacities in the anodic and cathodic scan ( $Q_{anodic}$  and  $Q_{cathodic}$ ) respectively) should be equal, and the ratio  $Q_{\text{anodic}}/Q_{\text{cathodic}}$  is unity. When irreversible processes contribute to the anodic capacity at higher potentials, this ratio deviates positively from unity. The increase beyond unity is defined as the irreversibility of the system, denoted as  $\rho$ :

$$\rho = Q_{\text{anodic}}/Q_{\text{cathodic}} - 1 \tag{1}$$

 $Q_{\text{anodic}}$  is the sum of the Faradaic  $(Q_F)$  and non-Faradaic  $(Q_{nF})$ capacities. Assuming oxidative decomposition of the electrolyte is completely irreversible, the cathodic capacity is purely non-Faradaic ( $Q_{\text{cathodic}} = Q_{\text{nF}}$ ). Limiting the amount of oxidation in the anodic scan to prevent electrode passivation, the non-Faradaic capacitive capacity in the anodic and cathodic scans should be equal. In this case, the expression for irreversibility becomes

$$\rho = Q_F / Q_{nF} \tag{2}$$

This shows that  $\rho$  is a measure of the extent of oxidation referenced to the capacitive, non-Faradaic charge and will increase with higher  $E_{\rm cutoff}$  as more oxidative decomposition occurs. For practical application of this metric, additional corrections are needed to account for minor irreversibility in the capacitive capacities. Experiments must be designed to limit the extent of irreversible oxidation, which could potentially passivate the active area of the electrode. A similar phenomenon of working electrode passivation with polymer electrolytes was observed by Hallinan et al. in 2016.<sup>32</sup> In this work, the oxidation content is checked by converting the irreversible capacity to the ratio of oxidized chain segments. A fresh cell is needed for measurements at each incremented cutoff potential to avoid accumulation of the oxidation product and to provide a pristine, unperturbed electrolyte/working electrode interface. Also, the significant amount of carbon in the sample may form percolation pathways and introduce nonnegligible leakage current especially at temperatures that exceed the melting temperature of semicrystalline polymers (30-50 °C for PEO:LiTFSI). At these temperatures, polymer creep is possible. Thus, for any cell configuration, experiments are needed to determine the irreversibility of non-Faradaic capacitances, or  $\rho_{\rm C}$ :

$$\rho_{\rm C} = Q_{\rm CA}/Q_{\rm CC} \tag{3}$$

Q<sub>CA</sub> and Q<sub>CC</sub> are the capacitive charges during anodic and cathodic scans, respectively.  $\rho_{\rm C}$  can be obtained by cycling the cell at potentials where electrolyte oxidation does not occur.

The irreversibility of a cell due to Faradaic reactions ( $\rho_{\rm F}$ ) is found by subtracting the premeasured capacitive irreversibility from the overall irreversibility, or  $\rho_{\rm F} = \rho - \rho_{\rm C}$ . If all prerequisites are met in the experiment,  $\rho_{\rm F}$  is independent of both the absolute value of the current density and the shape of the voltammogram, and thus the systematic error observed in the LSV method is eliminated. Also, because this method can be applied to irreversible oxidation, it provides some benefits over other cyclic voltammetry methods that assess stability through the detection of the subsequent reduction of the oxidation products in the cathodic scan. These CV methods have been successfully employed for solid sulfide electrolytes (LGPS, Li<sub>6</sub>PS<sub>5</sub>Cl, etc.) by detecting the reduction of polysulfide  $(S_x^{2-})$  generated during oxidation but are expected to have less utility for polymer electrolytes where oxidation is irreversible.2

Although the scanning rate should have less influence on this method compared to current density-based methods, it remains an important consideration due to the precision of the measurement. According to Nicholson et al., the Faradaic current of an irreversible system under linear sweep is proportional to  $v^{1/2}$ , where v is the scanning rate.<sup>26</sup> The capacitive charging current is proportional to v. Thus, the "signal to background" ratio  $(i_{\rm F}/i_{\rm nF})$  decreases with increased scanning rate, and a relatively low scanning rate is preferable. A slow rate (0.1 mV/s) was used in this work.

While the method is universal, polymer electrolytes present the challenge of low current densities, also compromising the sensitivity of the approach. Han et al. showed that incorporating conductive carbon into solid electrolyte materials, such as LLZO and LGPS, to increase the electrochemically active surface area of the working electrode enhances the sensitivity of voltammetry measurements, resulting in improved characterization of electrochemical stability. <sup>18</sup> Similarly, we blended a large quantity of graphite powder into our polymer electrolytes to expand the effective working electrode area, making the sample both ionically and electrically conductive. This study demonstrates the reversibility test on PEO and HNBR-based electrolytes. However, it should be broadly applicable to many polymer electrolyte compositions. As will be demonstrated, the dispersion of graphite throughout the polymer electrolyte is critical to enhance the sensitivity of the method, limiting the method to materials that are solution processable into free-standing graphite-filled composites, which complicates its application toward highly cross-linked materials and most gel electrolytes. Also, the ability of the method to provide accurate results for block copolymers is an open question, as surface interactions may lead to preferential wetting by one block. In principle, this method should be extendable to other classes of electrolytes such as sulfides and oxides, assuming that the materials are stable with graphite and can be readily processed into a composite. The high temperature sintering often needed for oxide electrolytes is likely to result in chemical redox reactions with the carbon, and alternative fillers such as platinum powder may be required.<sup>18</sup>

## 3. MATERIALS

To develop and validate the electrochemical reversibility test. PEO was chosen as the model material because (1) it is a wellestablished material, being among the first reported polymeric lithium ion conductors, (2) the simple linear structures is amenable to relatively straightforward structural analysis by accessible characterization techniques such as NMR and size exclusion chromatography (SEC), and (3) it and its derivatives (based on the ethylene oxide motif) still offer some of the highest reported room temperature conductivities.<sup>33–35</sup> Given these high conductivities, PEO-based analogues have found applications in commercial solid-state batteries for electric vehicles, such as the Bolloré Bluecar manufactured by Véhicule Electriques Pininfarina Bolloré. To demonstrate the versatility of this capacity-based method, a more oxidatively stable, nonether polymer electrolyte, namely, hydrogenated nitrile butadiene rubber complexed with LiTFSI salt (HNBR:LiTF-SI), was characterized. In 2019, we reported the key physical and electrochemical properties of this polymer electrolyte along with its plasticized formulations as potential electrolytes for lithium batteries with oxidative and thermal stability superior to PEO:LiTFSI. 10,36 Herein, the reversibility test is employed to confirm these previous findings, which relied upon the LSV method. Also, because  $\rho$  does not depend on the absolute current density but rather the ratio of capacities, we believe it will provide a fairer comparison to PEO, which has a higher ionic conductivity than the HNBR electrolytes.

### 4. PROCEDURE

To establish a quantitative description of PEO's oxidative stability over a potential range (3.5–4.2 V vs Li/Li<sup>+</sup>) relevant to state-of-the-art lithium-ion cells, a custom designed cell (Figure 3) for moisture/oxygen-free testing outside of the

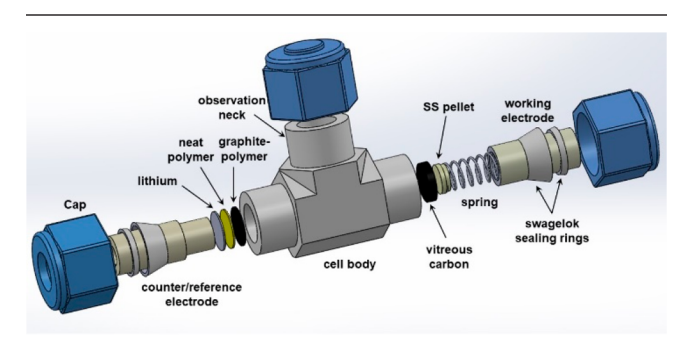


**Figure 3.** Schematic of electrochemical cell hardware employed for air- and moisture-free encapsulation of the materials. The cell body is based on commercially available Swagelok products, but custom stainless-steel rods were employed.

glovebox was employed. A cell consisting of the lithium metal, polymer electrolyte, and vitreous carbon working electrode was sealed between a spring-mounted stainless pellet and a cylindrical stainless counter/reference electrode. To prepare the cell, a polished vitreous carbon working electrode, a solution casted graphite infused PEO film (PEO:LiTFSI:graphite = 21.5:14.0:64.5 by mass), a carbon-free electrolyte film with an identical composition, and a lithium counter/reference electrode are laminated by hand. The HNBR cell is prepared by a similar procedure. Vitreous carbon essentially functions as a current collector but is also used to avoid potential corrosion of the stainless-steel cell parts at high

potentials. Moreover, its surface is easily polished between the measurements needed for sample-to-sample reproducibility. Li metal is a conventional reference electrode in the field, especially with solid electrolytes. To accommodate potential chemical reactions of the Li metal with the electrolytes, the cells are rested at the test temperature until the open circuit voltage stabilizes. It is assumed that the small current density during the CV tests does not substantially alter the Li/electrolyte interphase.

Polymer electrolyte films were prepared in large batches and stored in an argon filled glovebox ( $\rm H_2O$  and  $\rm O_2 < 0.4$  ppm) to ensure reproducibility between individual measurements. To enhance the conductivity of the polymer and electrode kinetics, all experiments were performed at an elevated temperature (60 °C for PEO and 70 °C for HNBR). The working electrode is slowly scanned (0.1 mV/s) between 3.0 V vs Li/Li<sup>+</sup> and  $E_{\rm cutoff}$  and  $\rho$  was determined through integration of the anodic and cathodic current. For PEO,  $E_{\rm cutoff}$  ranged from 3.5 to 4.2 V vs Li/Li<sup>+</sup>; a total of 8 samples were analyzed. For HNBR,  $E_{\rm cutoff}$  ranged from 3.6 to 4.6 V; a total of 7 samples were analyzed.

As discussed in the theory section, the reversibility test is based on analyzing a deviation from a reversible capacitive process. Thus, a closed voltammogram envelope is required for calculating the irreversibility. A closed envelope develops when the end of the CV test returns the system to its initial state, indicating good overall reversibility. However, the first CV cycle is disturbed by initial transient processes, such as the establishment of a concentration gradient, and does not form a closed envelope. Thus, the first cycle data was discarded, and the capacities in the second cycle were integrated to calculate the irreversibility. The stability—potential observations from the reversibility test were further supported with complementary structural characterization, including size exclusion chromatography (SEC) and nuclear magnetic resonance (NMR).

## 5. RESULTS AND DISCUSSION

Figure 2b shows the voltammogram of PEO scanned at 60 °C. At  $E_{\text{cutoff}} \leq 3.6 \text{ V}$ , the voltammogram is nearly symmetric, representative of an electrolytic capacitor. In the range of  $E_{\text{cutoff}}$ ≤ 4.2 V vs Li/Li<sup>+</sup>, no Faradaic peaks are observed in the voltammograms, including in the cathodic scan. These voltammograms satisfy the requirement of a non-Faradaic cathodic scan in the theoretical underpinnings described for this method. Yet as  $E_{\text{cutoff}}$  is incremented to higher potentials, the anodic current density increases relative to cathodic current density, suggesting the contribution of decomposition reactions. Thus,  $\rho$  also increases with  $E_{\rm cutoff}$  above 3.6 V vs Li/  $Li^+$ . As  $E_{\text{cutoff}}$  is increased to 4.6 V vs  $Li/Li^+$ , intercalation of the TFSI<sup>-</sup> anion into graphite is expected, and a broad peak due to intercalation can be observed in the cathodic scan (Figure S3).<sup>37</sup> This marks the upper limit of using the reversibility test on PEO:LiTFSI electrolytes, where the assumption  $Q_{cathodic}$  =  $Q_{nF}$  is no longer accurate.

The voltammograms in Figure 2b were integrated to provide the relationship between  $\rho$  and  $E_{\rm cutoff}$  in Figure 4. The  $\rho$ - $E_{\rm cutoff}$  relationship has two regions with distinct behavior: a constant  $\rho$  region ( $E_{\rm cutoff} \leq 3.6$  V vs Li/Li<sup>+</sup>), where  $\rho$  remains unchanged at  $\rho$  = 0.056, and a region where  $\rho$  monotonically increases ( $E_{\rm cutoff} > 3.6$  V). The invariant  $\rho$  at the lower potentials is consistent with the voltammograms being primarily capacitive in nature, and the polymer electrolyte is

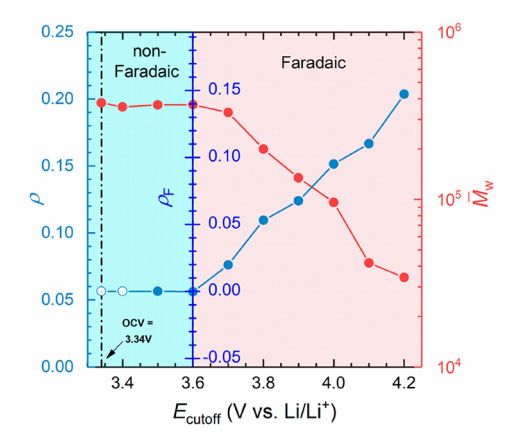


Figure 4. Irreversibility  $(\rho)$  and Faradaic irreversibility  $(\rho_{\rm F})$  of PEO:LiTFSI:graphite = 21.5:14.0:64.5 (by mass) sample obtained by integrating cyclic voltammograms of PEO:LiTFSI at incremented cutoff potentials and weight-average molar masses  $(\overline{M}_{\rm W})$  after equilibrating PEO:LiTFSI at the corresponding  $E_{\rm cutoff}$  for 24 h at 60 °C

concluded to be electrochemically stable over this potential range. Thus, the values of  $\rho$  in this region are used to establish  $\rho_{\rm C}$  for the experimental conditions. Above 3.6 V,  $\rho$  monotonically increases with  $E_{\rm cutoff}$  which is expected since the Faradaic current from oxidative reactions is more prominent in the voltammograms at the higher cutoff potential. Subtracting  $\rho_{\rm C}$  from  $\rho$ , the Faradaic irreversibility  $\rho_{\rm F}$  increases from 0 (3.6 V) to 0.16 (4.2 V). The stability threshold was taken at the potential where  $\rho_{\rm F}$  is increased by 0.01, or the contribution of the Faradaic reaction equals to 1% of the cathodic charge. For PEO:LiTFSI, the threshold is 3.6 V, which is considerably lower than in previous studies that report the oxidative stability to be above 3.8 V vs Li/Li<sup>+</sup>.9-16

To confirm that  $\rho_{\rm F}>0.01$  is indicative of irreversible oxidation reactions of the PEO electrolyte at high potentials, the samples were characterized by size exclusion chromatography. A series of PEO electrolytes were held at cutoff potentials from 3.4 V to 4.2 V vs Li/Li^+ for 24 h. The 24 h duration was to ensure that the electrode had equilibrated. After the test, the cells were opened inside the glovebox; the graphite-infused sample was peeled off with a razor blade, dissolved in DMF, and filtered to create a size exclusion

chromatography (SEC) sample. The resulting SEC characterizations are presented alongside  $\rho$  in Figure 4. Weight-average molar masses were calculated by comparison to calibration curves created with narrow PEO standards.

The SEC data largely confirms the conclusions from the voltammetry analysis. In the stable region ( $E_{\rm cutoff} \leq 3.6~{\rm V}$  vs Li/Li<sup>+</sup>),  $\bar{M}_{\rm W}$  of the sample remains unchanged, suggesting little oxidation has occurred. Thus, both  $\rho$  and  $\bar{M}_{\rm W}$  suggests that the absolute anodic stability threshold of PEO is approximately 3.6 V vs Li/Li<sup>+</sup>. In the unstable region,  $\bar{M}_{\rm W}$  of PEO decreases from  $3.7 \times 10^5$  (OCV, 3.6 V) to  $3.4 \times 10^4$  (4.2 V) or by a factor of 11. The monotonically decreasing  $\bar{M}_{\rm W}$  suggests an increased amount of chain scission, which is the major form of oxidative damage on PEO. <sup>38</sup> Decomposition of the PEO electrolyte at an elevated voltage was reported recently by Kobayashi et al. They found that branched PEO cycled with Li[Ni<sub>1/3</sub>Mn<sub>1/3</sub>Co<sub>1/3</sub>]O<sub>2</sub> (NMC333) between 2.7 and 4.2 V undergoes a reduction of  $\bar{M}_{\rm W}$  from 1.5 × 10<sup>6</sup> to 1.2 × 10<sup>5</sup> (factor of 12) during extended cycling. <sup>39</sup>

The SEC result confirms that (1) the oxidative current irreversibly degrades the PEO at potentials above 3.6 V and (2) the extent of oxidation is correlated to the cutoff potential. The necessity of adding graphite into the polymer sample can also be assessed by SEC.  $\bar{M}_{\rm W}$  of the graphite-free PEO sample oxidized at 4.2 V was relatively unchanged over 24 h  $(\overline{M}_{W}(\text{oxidized}):\overline{M}_{W}(\text{pristine}) = 0.98:1)$ . In comparison, the molecular weight of PEO in the graphite infused sample decreased by over 1 order of magnitude, or  $\overline{M}_{W}(\text{oxidized}):\overline{M}_{W}(\text{pristine}) = 0.09:1 \text{ (Figure S4)}.$  The difference is due to the additional electrochemically active surface area of the working electrode, which increases the fraction of the polymer in the electrode participating in the electrochemical oxidation. Without the high surface area from the graphite, an insignificant mass of polymer is oxidized, which cannot be readily detected via standard characterization approaches. For example, NMR fails to detect the oxidation of the neat PEO sample at 4.6 V vs Li/Li<sup>+</sup>. Even if graphite was added in the sample, the new proton signal of the oxidation product cannot be found in the <sup>1</sup>H NMR spectrum (Figure S5). <sup>1</sup>H NMR only begins to show a difference at 4.6 V vs Li/  $Li^+$  through the line shape change of  $\delta = 3.58$  ppm for the [-CH<sub>2</sub>O-] peak (Figure S6).

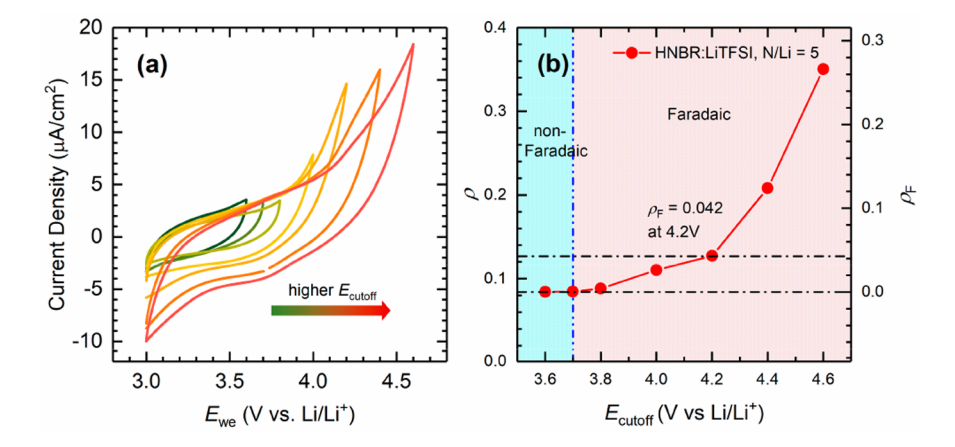


Figure 5. Reversibility characterization of HNBR:LiTFSI (HNBR:LiTFSI:graphite = 22.6:9.5:67.9 by mass) at 70 °C. (a) Cyclic voltammogram of HNBR:LiTFSI (N/Li = 5) scanned from 3.0 V vs Li/Li<sup>+</sup> to various  $E_{\rm cutoff}$  values at a scan rate of 0.1 mV/s and (b)  $\rho$  derived by integrating the corresponding voltammograms.

Figure 4 also shows that  $\rho$  does not converge to zero in the electrochemically stable region, suggesting the presence of a non-negligible leakage current. By holding the cell at 3.5 V for 24 h, we were able to confirm that the leakage current of the setup is in the vicinity of  $i_L = 0.1 \mu A$ . The leakage capacity during the reversibility test can be estimated by the leakage current integrated over the duration of the test  $(i_L \times t_{scan}) = 0.1$  $\mu$ A × 10000 s = 1 mC. The estimated leakage capacity is in good agreement with the irreversible capacity in the electrochemically stable region, which is also ~1 mC. Additional evidence is provided by the room temperature cycling of the cell. The  $i_1$  is expected to be near zero since the cell temperature is below the melting point of PEO:LiTFSI (typically above 30 °C), and the creep of the polymer electrolyte is slowed. We observed that  $\rho$  converges to near 0 at room temperature (25 °C), further confirming that  $\rho_C$  is mainly caused by the electronic leakage current in the setup (Figure S7a).

To assess the versatility of the electrochemical reversibility method, HNBR:LiTFSI was also characterized, which is a more oxidatively stable, nitrile-based polymer electrolyte. The reversibility results for HNBR:LiTFSI with N/Li = 5 are presented in Figure 5. The characterization was done at 70 °C to increase the electrode conductivity and electrode kinetics, while being consistent with previous experimental parameters. Figure 5a provides the incremented voltammograms from 3.6 to 4.6 V vs Li/Li<sup>+</sup>. At low E<sub>cutoff</sub>, the voltammograms are largely capacitive. Obvious oxidative current is not observed during the scan. The irreversibility values derived by integrating the voltammogram are shown in Figure 5b. A constant  $\rho$  which corresponds to  $\rho_{\rm C}$  (caused by leakage current) can also be found at ≤3.7 V vs Li/Li<sup>+</sup>, consistent with our observation in the PEO system. Applying the  $\rho_{\rm F}$  = 0.01 criterion, the stability threshold of HNBR is assigned to 3.7 V vs Li/Li<sup>+</sup>. Similar to PEO, we found that  $ho_{
m C}$  in the HNBR system is also temperature-dependent, converging to ~0 at room temperature (Figure S7b).

In the electrochemically unstable region,  $\rho_{\rm F}$  monotonically increases with  $E_{\rm cutoff}$  reaching 0.042 at 4.2 V vs Li/Li<sup>+</sup>. In comparison,  $\rho_{\rm F}$  of PEO at 4.2 V was 0.16, indicating that HNBR is considerably more stable than PEO. Reversibility tests not only offer a comparison of the decomposition onset between HNBR and PEO but also proves that the nitrile-bearing structure is more resistant to oxidation even above the threshold, supporting our previous conclusions about the superior anodic stability of saturated nitrile bearing polymer electrolytes.

However, the  $\overline{M}_{\rm W}$ – $E_{\rm cutoff}$  relationship of HNBR cannot be validated with SEC. HNBR has a cross-linked and branched structure, which limits its solubility in common SEC mobile phases. Second, unlike PEO, oxidation of HNBR does not necessarily result in chain scission and commensurate  $\overline{M}_{\rm W}$  reduction. Polymers with a saturated hydrocarbon backbone are often oxidized at their pendant groups or through hydrogen abstraction from the backbone. Cross-linked polymers and polymer gels are expected to suffer from many of these same problems, making SEC unsuitable for characterizing oxidation. Thus, the reversibility test provides a feasible alternative for these materials, while addressing some of the inherent limitations of LSV.

In conclusion, we established a sensitive, versatile electrochemical method to assess the electrochemical stability of polymer electrolytes. The method combines an established reversibility test with high surface area carbon composite working electrodes to provide a sensitive, internally referenced measure of irreversibility, allowing for comparison between polymer electrolyte materials with differing ionic conductivities. The high surface area provided by the dispersed carbon is critical to improving the resolution of the technique, and the ratio of Faradaic to non-Faradaic current  $(\rho)$  compensates for the commensurate increase in capacitance. Moreover, the reversibility test is compatible with polymeric materials with irreversible and/or complex oxidation behavior (beyond simple chain scission) or that are insoluble in conventional solvents, which otherwise complicates conventional structural analysis (e.g., SEC, light scattering, solution NMR). Using this method, the absolute anodic stability thresholds of PEO and HNBR were determined to be 3.6 and 3.7 V vs Li/Li<sup>+</sup>, respectively. These potentials should not be interpreted as operation voltage limits for these materials, above which solid state batteries cannot be operated, because electrode passivation and other physicochemical processes may provide practical kinetic stability. However, they clearly show that oxidative stability needs to be carefully considered and exhaustively studied at potentials exceeding these thresholds. Ultimately, practical stability will depend on the overall electrode formulation, with the active material strongly influencing the nature of the oxidation processes.<sup>41</sup>

## ASSOCIATED CONTENT

# Supporting Information

The Supporting Information is available free of charge at https://pubs.acs.org/doi/10.1021/acs.chemmater.0c04248.

Experimental methods, voltammogram of PEO at 4.6 V, SEC chromatogram of graphite free/infused sample, NMR results, irreversibility of PEO and HNBR at room temperature, and measurement of leakage current (PDF)

#### AUTHOR INFORMATION

# **Corresponding Author**

Wyatt E. Tenhaeff — Department of Chemical Engineering and Materials Science Program, University of Rochester, Rochester, New York 14627, United States; oorcid.org/0000-0001-7132-3171; Phone: (585)275-5080; Email: wyatt.tenhaeff@rochester.edu

## **Authors**

Zhuo Li — Department of Chemical Engineering, University of Rochester, Rochester, New York 14627, United States; orcid.org/0000-0002-8830-9891

Yineng Zhao — Materials Science Program, University of Rochester, Rochester, New York 14627, United States; orcid.org/0000-0002-8899-7663

Complete contact information is available at: https://pubs.acs.org/10.1021/acs.chemmater.0c04248

#### Notes

The authors declare no competing financial interest.

## ACKNOWLEDGMENTS

This material is based upon work supported by the National Science Foundation under Grant No. 1845805. The authors thank Dr. Shaofei Wang for many insightful discussions. The authors thank Mr. Clyde Overby and Dr. Danielle Benoit at

University of Rochester for the help with SEC. The authors thank Mr. Mitch Juneau, Mr. Xinquan Chen, and Miss Wenshi Zhang at University of Rochester for their help with BET and NMR tests.

#### ABBREVIATIONS

CV, cyclic voltammetry; HNBR, hydrogenated butadiene rubber; LSV, linear sweep voltammetry; LiTFSI, lithium bis(trifluoromethanesulfonyl) imide; NMR, nuclear magnetic resonance; PEO, poly(ethylene oxide); SEC, size exclusion chromatography

#### REFERENCES

- (1) Kraytsberg, A.; Ein-Eli, Y. Higher, Stronger, Better. A Review of 5 V cathode materials for advanced lithium-ion batteries. *Adv. Energy Mater.* **2012**, *2*, 922–939.
- (2) Fergus, J. W. Recent developments in cathode materials for lithium ion batteries. *J. Power Sources* **2010**, *195*, 939–954.
- (3) Li, Q.; Wang, Y.; Wang, X.; Sun, X.; Zhang, J. N.; Yu, X.; Li, H. Investigations on the fundamental process of cathode electrolyte interphase formation and evolution of high-voltage cathodes. *ACS Appl. Mater. Interfaces* **2020**, *12*, 2319–2326.
- (4) Dupré, N.; Cuisinier, M.; Legall, E.; War, D.; Guyomard, D. Contribution of the oxygen extracted from overlithiated layered oxides at high potential to the formation of the interphase. *J. Power Sources* **2015**, 299, 231–240.
- (5) Assat, G.; Iadecola, A.; Foix, D.; Dedryvère, R.; Tarascon, J.-M. Direct quantification of anionic redox over long cycling of Li-rich NMC via hard X-ray photoemission spectroscopy. *ACS Energy Lett.* **2018**, 3, 2721–2728.
- (6) Lotsch, B. V.; Maier, J. Relevance of solid electrolytes for lithium-based batteries: a realistic view. *J. Electroceram.* **2017**, 38, 128–141.
- (7) Wang, H.; Wang, Q.; Cao, X.; He, Y.; Wu, K.; Yang, J.; Zhou, H.; Liu, W.; Sun, X. Thiol-branched solid polymer electrolyte featuring high strength, toughness, and lithium ionic conductivity for lithiummetal batteries. *Adv. Mater.* **2020**, *32*, 2001259.
- (8) Mousavi, M. P. S.; Dittmer, A. J.; Wilson, B. E.; Hu, J.; Stein, A.; Buhlmann, P. Unbiased quantification of the electrochemical stability limits of electrolytes and ionic liquids. *J. Electrochem. Soc.* **2015**, *162*, A2250—A2258.
- (9) Xi, J.; Qiu, X.; Cui, M.; Tang, X.; Zhu, W.; Chen, L. Enhanced electrochemical properties of PEO-based composite polymer electrolyte with shape-selective molecular sieves. *J. Power Sources* **2006**, *156*, 581–588.
- (10) Li, Z.; Zhao, Y.; Tenhaeff, W. E. 5 V stable nitrile-bearing polymer electrolyte with aliphatic segment as internal plasticizer. *ACS Appl. Energy Mater.* **2019**, *2*, 3264–3273.
- (11) Park, C. H.; Kim, D. W.; Prakash, J.; Sun, Y.-K. Electrochemical stability and conductivity enhancement of composite polymer electrolytes. *Solid State Ionics* **2003**, *159*, 111–119.
- (12) Shin, J.-H.; Henderson, W. A.; Passerini, S. PEO-based polymer electrolytes with ionic liquids and their use in lithium metal-polymer electrolyte batteries. *J. Electrochem. Soc.* **2005**, *152*, A978—A983.
- (13) Sylla, S.; Sanchez, J.-Y.; Armand, M. Electrochemical study of linear and crosslinked POE-based polymer electrolytes. *Electrochim. Acta* **1992**, *37*, 1699–1701.
- (14) Zhai, H.; Gong, T.; Xu, B.; Cheng, Q.; Paley, D.; Qie, B.; Jin, T.; Fu, Z.; Tan, L.; Lin, Y. H.; Nan, C. W.; Yang, Y. Stabilizing polyether electrolyte with a 4 V metal oxide cathode by nanoscale interfacial coating. ACS Appl. Mater. Interfaces 2019, 11, 28774—28780.
- (15) Cheng, H.; Zhu, C.; Huang, B.; Lu, M.; Yang, Y. Synthesis and electrochemical characterization of PEO-based polymer electrolytes with room temperature ionic liquids. *Electrochim. Acta* **2007**, *52*, 5789–5794.

- (16) Hallinan, D. T.; Balsara, N. P. Polymer electrolytes. *Annu. Rev. Mater. Res.* **2013**, 43, 503–525.
- (17) Jalem, R.; Morishita, Y.; Okajima, T.; Takeda, H.; Kondo, Y.; Nakayama, M.; Kasuga, T. Experimental and first-principles DFT study on the electrochemical reactivity of garnet-type solid electrolytes with carbon. *J. Mater. Chem. A* **2016**, *4*, 14371–14379.
- (18) Han, F.; Zhu, Y.; He, X.; Mo, Y.; Wang, C. Electrochemical stability of Li<sub>10</sub>GeP<sub>2</sub>S<sub>12</sub> and Li<sub>7</sub>La<sub>3</sub>Zr<sub>2</sub>O<sub>12</sub> solid electrolytes. *Adv. Energy Mater.* **2016**, *6*, 1501590.
- (19) Ohta, S.; Kobayashi, T.; Asaoka, T. High lithium ionic conductivity in the garnet-type oxide  $Li_{7-X}La_3(Zr_{2-X}, Nb_X)O_{12}$  (X = 0–2). *J. Power Sources* **2011**, 196, 3342–3345.
- (20) Kotobuki, M.; Kanamura, K.; Sato, Y.; Yoshida, T. Fabrication of all-solid-state lithium battery with lithium metal anode using  $Al_2O_3$ -added  $Li_7La_3Zr_2O_{12}$  solid electrolyte. *J. Power Sources* **2011**, 196, 7750–7754.
- (21) Dewald, G. F.; Ohno, S.; Kraft, M. A.; Koerver, R.; Till, P.; Vargas-Barbosa, N. M.; Janek, J.; Zeier, W. G. Experimental assessment of the practical oxidative stability of lithium thiophosphate solid electrolytes. *Chem. Mater.* **2019**, *31*, 8328–8337.
- (22) Kamaya, N.; Homma, K.; Yamakawa, Y.; Hirayama, M.; Kanno, R.; Yonemura, M.; Kamiyama, T.; Kato, Y.; Hama, S.; Kawamoto, K.; Mitsui, A. A lithium superionic conductor. *Nat. Mater.* **2011**, *10*, 682–6.
- (23) Xu, K.; Ding, S. P.; Jow, T. R. Toward reliable values of electrochemical stability limits for electrolytes. *J. Electrochem. Soc.* **1999**, *146*, 4172–4178.
- (24) Xu, K.; Ding, M. S.; Richard Jow, T. A better quantification of electrochemical stability limits for electrolytes in double layer capacitors. *Electrochim. Acta* **2001**, *46*, 1823–1827.
- (25) Olson, E. J.; Buhlmann, P. Unbiased assessment of electrochemical windows: minimizing mass transfer effects on the evaluation of anodic and cathodic limits. *J. Electrochem. Soc.* **2013**, *160*, A320—A323
- (26) Nicholson, R. S.; Shain, I. Theory of stationary electrode polarography. *Anal. Chem.* **1964**, *36*, 706–723.
- (27) Capiglia, C.; Saito, Y.; Kageyama, H.; Mustarelli, P.; Iwamoto, T.; Tabuchi, T.; Tukamoto, H. <sup>7</sup>Li and <sup>19</sup>F diffusion coefficients and thermal properties of non-aqueous electrolyte solutions for rechargeable lithium batteries. *J. Power Sources* **1999**, *81*–*82*, 859–862.
- (28) Hayamizu, K.; Aihara, Y.; Arai, S.; Martinez, C. G. Pulegradient spin-echo <sup>1</sup>H, <sup>7</sup>Li, and <sup>19</sup>F NMR diffusion and ionic conductivity measurements of 14 organic electrolytes containing LiN(SO<sub>2</sub>CF<sub>3</sub>)<sub>2</sub>. *J. Phys. Chem. B* **1999**, *103*, 519–524.
- (29) Gorecki, W.; Jeannin, M.; Belorizky, E.; Roux, C.; Armand, M. Physical properties of solid polymer electrolyte PEO(LiTFSI) complexes. J. Phys.: Condens. Matter 1995, 7, 6823–6832.
- (30) Fischer, E.; Kimmich, R.; Beginn, U.; Möller, M.; Fatkullin, N. Segment diffusion in polymers confined in nanopores: a fringe-field NMR diffusometry study. *Phys. Rev. E: Stat. Phys., Plasmas, Fluids, Relat. Interdiscip. Top.* **1999**, *59*, 4079–4084.
- (31) Weingarth, D.; Noh, H.; Foelske-Schmitz, A.; Wokaun, A.; Kötz, R. A reliable determination method of stability limits for electrochemical double layer capacitors. *Electrochim. Acta* **2013**, *103*, 119–124.
- (32) Hallinan, D. T.; Rausch, A.; McGill, B. An electrochemical approach to measuring oxidative stability of solid polymer electrolytes for lithium batteries. *Chem. Eng. Sci.* **2016**, *154*, 34–41.
- (33) Fenton, D. E.; Parker, J. M.; Wright, P. V. Complexes of alkali metal ions with poly(ethylene oxide). *Polymer* 1973, 14, 589.
- (34) Hallinan, D. T.; Villaluenga, I.; Balsara, N. P. Polymer and composite electrolytes. MRS Bull. 2018, 43, 759–767.
- (35) Motavalli, J. A Solid Future. Nature 2015, 526, S96-S97.
- (36) Zhao, Y.; Tenhaeff, W. E. Thermally and oxidatively stable polymer electrolyte for lithium batteries enabled by phthalate plasticization. *ACS Appl. Polym. Mater.* **2020**, *2*, 80–90.
- (37) Qi, X.; Blizanac, B.; DuPasquier, A.; Meister, P.; Placke, T.; Oljaca, M.; Li, J.; Winter, M. Investigation of PF6(-) and TFSI(-) anion intercalation into graphitized carbon blacks and its influence on

high voltage lithium ion batteries. Phys. Chem. Chem. Phys. 2014, 16, 25306-13.

- (38) Decker, C. Radiation-induced oxidation of solid poly(ethylene oxide). II. mechanism. *J. Polym. Sci.: Polym. Chem.* **1977**, *15*, 799–813.
- (39) Kobayashi, T.; Kobayashi, Y.; Tabuchi, M.; Shono, K.; Ohno, Y.; Mita, Y.; Miyashiro, H. Oxidation reaction of polyether-based material and its suppression in lithium rechargeable battery using 4 V class cathode,  $\text{LiNi}_{1/3}\text{Mn}_{1/3}\text{Co}_{1/3}\text{O}_2$ . ACS Appl. Mater. Interfaces 2013, 5, 12387–93.
- (40) Geuskens, G.; Baeyens-Volant, D.; Delaunois, G.; Lu Vinh, Q.; Piret, W.; David, C. Photo-oxidation of polymers-II. the sensitized decomposition of hydroperoxides. the main path for initiation of the photo-oxidation of polystyrene irradiated at 253.7nm. *Eur. Polym. J.* 1978, 14, 299–303.
- (41) Li, W.; Song, B.; Manthiram, A. High-voltage positive electrode materials for lithium-ion batteries. *Chem. Soc. Rev.* **2017**, *46*, 3006–3059.